EXPERIMENTAL VERIFICATION OF IDENTIFICATION ALGORITHMS FOR CONTROL OF FLEXIBLE STRUCTURES

B. Sridhar, J.-N Aubrun, and K. R. Lorell
Lockheed Palo Alto Research Laboratory
Palo Alto, CA 94304

ABSTRACT

This paper describes an on-going simple laboratory experiment, referred to as the Beam Control Experiment (BCE), which has the essential features of a large flexible structure. The experiment is used to develop and evaluate identification and control algorithms which look promising in the active control of high performance large space structures. Some results on the maximum likelihood identification of the parameters of the beam-actuator-sensor assembly from experimental data is presented in the paper.

I. INTRODUCTION

One of the major problems in the design of control systems which operate in the presence of a flexible structure is obtaining accurate information about the plant dynamics. In particular, knowledge of the frequencies, damping ratios and mode shapes of the flexible modes is critical to the successful design of a high performance system. System identification is an iterative process, the success of which depends upon the choice of algorithm and system model, the choice of inputs to excite the system, and the quality of output data. A careful integration of these items is especially critical in the case of large flexible structures.

In this paper we describe the development and performance testing of a simple laboratory model of a jitter control system designed to provide a stable image with optical components mounted on a flexible structure. The study will be carried out in three stages: (a) identification with simulated data, (b) identification with real data, and (c) comparison of closed loop performance with simulated results. Results from the first two stages are reported in this paper.

This paper is organized as follows: Section 2 describes the experimental set-up and a mathematical model for the BCE is developed in Section 3. A brief description of the maximum likelihood estimation (MLE) algorithm is presented in Section 4. Results on the identification of the parameters of the BCE using both simulated and experimental data are discussed in Section 5. A summary and future work is described in Section 6.

II. BEAM CONTROL EXPERIMENT

The idea behind this experiment (Fig. 1) is to demonstrate the interaction between the control of an optical system, symbolized by a laser beam, and control of a flexible structure, represented by a flexible aluminum beam to which passive and active mirrors are attached. These mirrors bounce the laser beam toward a desired target. The interesting control problem stems

from the fact that the active mirror is in fact part of a proof-mass actuator. Thus, any attempt to control the laser beam will tend to disturb the aluminum beam, thereby also disturbing the laser beam. This intricate coupling is quite a challenge for a classical design but more amenable to modern techniques. The other aspect of the experiment is the use of a commercially available cated microprocessor (ISI MCP-100) capable of handling at maximum a 32-[illegible] e Kalman filter at a 2000-Hz sampling rate. Such implementation, aside f[illegible] its laboratory usefulness, bring control technology one step further toward real space implementation, and the experience gained is valuable.

The schematic of the experiment is shown in Figs. 2 and 3. The laser beam bounces first on a mirror situated near the middle point of the vertical aluminum beam, then on a mirror attached to the tip of a pivoted proof-mass actuator (PPM). The laser beam finally reaches a photodetector, which measures the laser beam position. A beam splitter provides a visual display of the jitter by projecting the spot on a remote screen.

Two sensors are used in the experiment: the photodetector measuring the line-of-sight (LOS) error, and the PPM rate sensor measuring the relative velocity of the proof-mass.

A preliminary experiment had been performed earlier (Ref. 1) using commercially available software for identification and control synthesis. Only one sensor was used (position) and the control system was able to significantly damp out the beam vibrations; thus stabilizing the line-of-sight. However, in order to eliminate the static error and achieve a higher performance, a better model is needed and thus more sophisticated identification techniques are sought to that end.

For purposes of identification, a known control force is applied to the beam using the proof-mass actuator. The control force time-history and the beam position and relative rate outputs are recorded on a Nicolet 4094 digital oscilloscope. Special software transfers the input and output data from the Nicolet 4094 to a Harris 800 computer where the identification algorithms were exercized. Thus an efficient link between hardware te[illegible]s and sophisticated computer analyses (Fig. 4) was established.

III. MATHEMATICAL MODEL

In this Section, a state space model of the system is developed. The mathematical form of this model will be used both for simulation and identification of the parameters of the BCE.

The angular displacement, θ_a, of the proof-mass actuator is limited to to a few degrees. For small angles the force and torque applied by the actuator are given by the equations (Reference 2)

$$T = I\ddot{\theta}_a \tag{1}$$

$$f_a = mb\ddot{\theta}_a \tag{2}$$

where m is the mass of the proof-mass actuator, b is the distance from the center of mass to the proof-mass pivot and I is the centroid inertia of the proof-mass actuator. The dynamics of the aluminum beam will be defined in terms of the principal modes and mode shapes. Let q_i be the modal amplitude of the i^{th} mode and define:

ω_i = angular velocity of the i^{th} mode

ζ_i = damping of the i^{th} mode

ϕ_i = translational mode shape of the i^{th} mode at the beam tip (where the PPM is mounted)

and ϕ_i^R = rotational mode shape of the i^{th} mode at this tip. Let ϕ_{im} and ϕ_{im}^R be the corresponding values for the mode shapes where the mirror is mounted on the flexible beam. The modal equations for the beam are:

$$\ddot{q}_i + 2\zeta_i \omega_i \dot{q}_i + \omega_i^2 q_i = -\phi_i f_a - \phi_i^R T \qquad i = 1,2,..M \quad (3)$$

where M is the number of modes represented in the model. Due to the actuator dynamics, the control force f_c applied to the actuator is related to f_a by the equation

$$rf_a = rf_c - (K + mgb)(\theta_a - \theta_t) - D(\dot{\theta}_a - \dot{\theta}_t) \qquad (4)$$

where r = lever arm of the actuator

g = acceleration due to gravity

K = spring constant of the actuator

D = damping constant of the actuator

and θ_t = rotation of the beam tip

The rotation of the beam tip can be expressed in terms of the modal amplitudes by

$$\theta_t = \sum_i^M \phi_i^R q_i \ . \qquad (5)$$

Equations (1) - (5) can be reduced to the set of equations

$$\ddot{\theta}_a = -(K + mgb)/I\ \theta_a - D/I\ \dot{\theta}_a + K/I\ \Sigma\ \phi_i^R\ q_i + D/I\ \Sigma\ \phi_i^R\ \dot{q}_i + \frac{r}{I}\ f_c \qquad (6)$$

and

$$\ddot{q}_i = -A_i\ \theta_a - C_i\ \dot{\theta}_a - 2\ \zeta_i\ \omega_i\ \dot{q}_i - \omega_i^2\ q_i + A_i\ \Sigma\ \phi_i^R\ q_i + C_i\ \Sigma\ \phi_i^R\ \dot{q}_i + B_i\ f_c \qquad (7)$$

where

$$A_i = -K\ (I\ \phi_i^R + mb\phi_i)/I \qquad (8)$$

$$B_i = A_i\ r/K \qquad (9)$$

and

$$C_i = A_i\ D/K \qquad (10)$$

Let y_1 be the displacement of the laser beam from the reference point (i.e., this is a measurement of the L.O.S. error). Let y_2 be the relative angular rate between the actuator and the beam tip. Then,

$$y_1 = 2\ \left[\Sigma\ \phi_{im}\ q_i - (\ell_1 + \ell_2)\ \Sigma\ \phi_{im}^R\ q_i + \ell_2\theta_a\right] \qquad (11)$$

and

$$y_2 = \dot{\theta}_a - \dot{\theta}_t = \dot{\theta}_a - \Sigma\ \phi_i^R\ q_i \qquad (12)$$

where ℓ_1 is the distance between the mirror on the beam and the mirror on the proof-mass actuator and ℓ_2 is the distance between the photodetector and the mirror on the proof-mass actuator (See Fig. 3).

Equations 6, 7, 11, and 12 give a state space representation of the input/output behavior of the BCE with $\left[\theta_a\ \dot{\theta}_a\ q_1\ \dot{q}_1\ \cdots\ q_M\ \dot{q}_M\right]$ as the state vector.

For a single mode model the equations are given by

$$\dot{x} = Fx + Gu \qquad (13)$$

$$y = Hx \qquad (14)$$

where

$$F = \begin{bmatrix} 0 & 1 & 0 & 0 \\ -\omega_a^2 & -D/I & \omega_2^2\,\phi_1^R & D/I\,\phi_1^R \\ 0 & 0 & 0 & 1 \\ -A_1 & -C_1 & -\omega_1^2+A_1\phi_1^R & C_1\phi_1^R - 2\,\zeta_1\omega_1 \end{bmatrix} \tag{15}$$

$$G = \begin{bmatrix} 0 & r/I & 0 & B_1 \end{bmatrix}^T \tag{16}$$

and

$$H = \begin{bmatrix} 2\,\ell_2 & 0 & 2\,(\phi_{1m} - (\ell_1 + \ell_2)\,\phi_{1m}^R) & 0 \\ 0 & 1 & 0 & -\phi_1^R \end{bmatrix} \tag{17}$$

where $\omega_a^2 = (K + mgb)/I$. (18)

Also, define $\zeta_a = \dfrac{D}{2\sqrt{I(K+mgb)}}$. (19)

The F, G and H matrices depend on the unknown parameters ($\omega_a, D, \omega_1, \zeta_1, \phi_1, \phi_1^R, \phi_{1m}, \phi_{1m}^R$) and the known parameters (I, m, b, r, ℓ_1 and ℓ_2). The values of the known parameters are tabulated in Table 1. In this model the number of unknown parameters is equal to (6M+2) where M is the number of modes.

I	$4X10^{-4}$ Kg-m^2
m	0.07895 Kg
b	0.06985 m
r	0.021 m
ℓ_1	0.165 m
ℓ_2	0.217 m

Table 1. Known Parameters of the BCE

IV. MAXIMUM LIKELIHOOD ESTIMATION (MLE)

There are several methods available for the estimation/identification of parameters Figure 6 shows the main components of an identification method. The system to be identified and a mathematical model, M(p), of the system is excited by a known input u. An error function, L(p,e), is formed from the outputs of the system and the model. Identification is the process of adjusting the model parameters p to minimize the error function. The choice of M(p), L(p,e) and the adjusting mechanism for p lead to different identification algorithms. In this paper, we shall restrict our attention to the maximum likelihood estimation of parameters.

The MLE can be applied to a large class of problems and has good statistical convergence and accuracy properties. In addition, MLE is well suited for identifying physical parameters of the system. This is a drawback with most recursive algorithms. The main disadvantage of MLE is the amount of computation. However, the amount of computation can be reduced significantly by taking into account the special features of the dynamics of the large space structures.

The flow of computation in the MLE is shown in Fig. 7. The mathematical model for the system is assumed to be

$$\dot{x} = F(p)\, x + G(p)u + \omega \tag{20}$$

$$y = H(p)\, x + \nu \tag{21}$$

where x is the n-dimensional state vector, y the p-dimensional output vector and u the m-dimensional input vector. ω and represent the process and measurement noise respectively. The matrices F, G and H depend on p, the vector of unknown system parameters. An input signal $[u(t),\ o < t < t_N]$ has been applied to the system and the output y of the system has been observed at discrete times $t_o, t_1, \ldots t_N$. Further, it is assumed that x(o) and ω are zero-mean gaussian random variables with

$$\text{cov}\ (x(o)) = P(o) \tag{22}$$

$$\text{cov}\ (\omega) = Q \tag{23}$$

and

$$\text{cov}\ (\nu) = R \tag{24}$$

The identification problem consists of estimating the parameters p from the experimental data $u(t_i)$, $y(t_i)$, $i = 1,2,\ldots N$. Let $\hat{x}$ be the state estimate, $\hat{y}$ the output estimate, and $e(t_R)$ be the output error

where

$$e(t_k) = y(t_k) - \hat{y}(t_k). \tag{25}$$

The negative log likelihood function, v(p,e), can be written as

$$V(p,e) = -\log L(p,e) = \sum_{i=1}^{N} \bar{e}(i)\, \bar{B}^{-1}(i)\, e(i) + \log |B(i)| \qquad (26)$$

The maximum likelihood estimate of the parameters p is obtained by maximizing the likelihood function L(p,e) (or by minimizing V(p,e)). This nonlinear minimization problem has to be solved by numerical methods and makes the MLE computationally intensive. The computational aspects of MLE are discussed in Reference 4.

V. IDENTIFICATION RESULTS

Numerical results on the identification of the parameters will be presented in two steps. First results from the identification of simulated data will be shown. This will be followed by results from experimental data.

a. Simulation Results: Identification with simulated data was done to get a better understanding of the dynamics of the BCE, to provide guidelines to set up the experiment and to test the MLE software. The system was simulated using 4 modes and was excited by a "bang-bang" type input with an amplitude of ±0.1 Newton. Figure 8 shows the laser beam position and relative velocity output from the simulation. This input/output simulated data was used to identify a single mode beam model of the system (see equations 13-17). The negative log likelihood function V(p,e) was probed at a few points to see its variation with parameter p. Figure 9 shows the variation of the likelihood surface with ω_a and ω_1. The surface is well-behaved in these two variables. The damping terms ζ_a and ζ_1 were set to the simulation values and only parameters (ω_a, ω_1, ϕ_1, ϕ_1^R, ϕ_{im} and ϕ_{im}^R) were allowed to vary. Table 2 shows the results based on simulated data. There is good agreement between simulated and estimated values. Now we are ready to try the identification with experimental data.

b. Experimental Results: The aluminum beam was excited by applying to the proof-mass actuator a sinusoidal force with a linearly varying frequency (so-called "chirp" excitation). Figure 10 shows the control force f_c. The position and rate measurements are shown in Figure 11. As before, the single mode model will be used as a starting point for the identification of parameters (ω_a, D, ω_1, ζ_1, ϕ_1, ϕ_1^R, ϕ_{im}, ϕ_{im}^R). Initially, the MLE had convergence problems. These were related to one or more of the following causes: 1) large differences between the values of some of the actual BCE parameters and those of the original simulation, 2) bias in the input force and position measurements, and 3) error in rate measurement calibration.

The bias was accounted for simply by subtracting a constant from the force input and position output. The error in rate calibration was taken into account by defining a scale factor α. This results in a new H matrix where

$$H = \begin{bmatrix} 2\ell_2 & 0 & 2(\phi_{im} - (\phi_{im} - (\ell_1+\ell_2)\,\phi^R_{im}) & 0 \\ 0 & \alpha & 0 & -\phi^R_1\,\alpha \end{bmatrix} \quad (27)$$

The scale factor was estimated along with the other 8 parameters. The estimated values are shown in Table 3. The model parameters shown in Table 3 for "simulation values" were obtained from an extremely simplified model of the aluminum beam (cantilevered with a point mass at tip). Thus, it is not surprising that some of the values obtained from the identification are very different. In particular, values of rotational mode shapes are quite sensitive to local inertias and masses.

Parameter	Simulated Data	Estimate (Simulation Data)	Estimate (Experimental Data)
ω_a	46.36	45.5	37.18
ω_1	54.63	54.58	40.32
ζ_a	0.005	.005*	85E-4
ζ_1	0.005	.005*	0.01
ϕ_1	3.328	3.49	7.48
ϕ_1	-13.51	-13.61	-110.0
ϕ_{im}	1.068	0.98	21.0
ϕ^R_{im}	-10.6	-10.3	2.49
α	1.0	1.0*	0.80

*These parameters were set to their simulation values.

Table 3 Results with Experimental Data

Figure 11 shows a comparison between the measured and estimated values of the outputs. The estimated values were generated for the prameter set which resulted from identification using experimental data (Table 3). Figure 11a shows the measured and estimated values of the position. Figure 11b is a blow-up of the same curve to show the difference between measured and estimated values. Figures 11c and 11d show curves similar to 11a and 11b for the rate measurement. There is very good agreement between the model output and the experimental data.

This model will be validated by taking the direct approach. In the third stage of the experiment, a control system will be designed using the identified model. The predicted behavior of the control system will be compared with its experimental behavior.

VI. CONCLUSIONS AND SUMMARY

In this paper, we have described a laboratory experiment which has the salient features of controlling an optical system located on a flexible structure. The experiment will be used as a test bed for designing control and identification algorithms for large space structures. The parameters of a model suitable for designing a control system were identified using maximum likelihood estimation. The real test of a model is of course how well it satisfies the goal of modelling. Currently, we are designing a control system based on this model and the results of this final stage will be reported in another paper.

VII. REFERENCES

1. S. C. Shah, R. A. Walker and D. B. Varvell, A Control Design Workstation, IEEE Control Systems Society Symposium on Computer-Aided Control System Design Sept. 28-30, 1983, Cambridge, Mass.

2. J.-N. Aubrun and G. Margulies, Low-Authority Control Synthesis for Large Space Structures, NASA Contractor Report NAS1-14887-Task 11 May 1982.

3. K. J Astrom, Maximum Likelihood and Prediction Error Methods, Automatica Vol. 16, pp 551-574, 1980.

4. N. K. Gupta and R. K. Mehra, Computational Aspects of Maximum Likelihood Estimation and Reduction in Sensitivity Function Calculations, IEEE Transactions on Automatic Control, AC-19, No. 6, 1974.

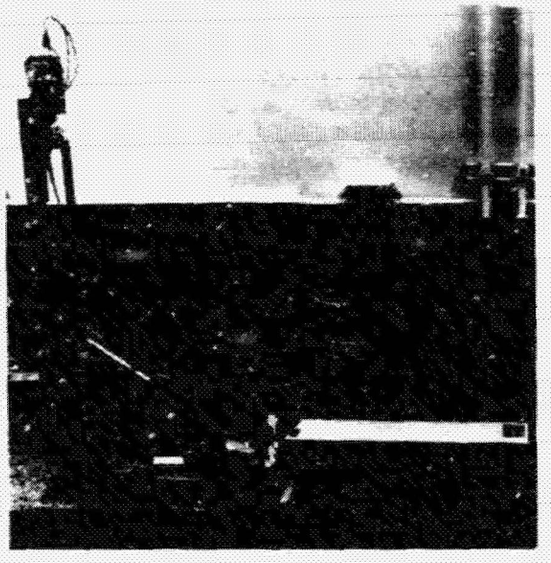

FIG. 1 BEAM CONTROL EXPERIMENT

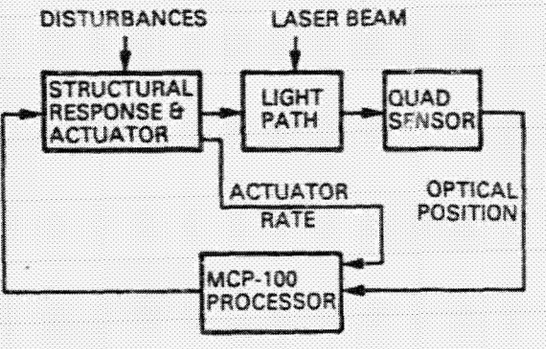

FIG. 3 BEAM CONTROL SCHEMATIC

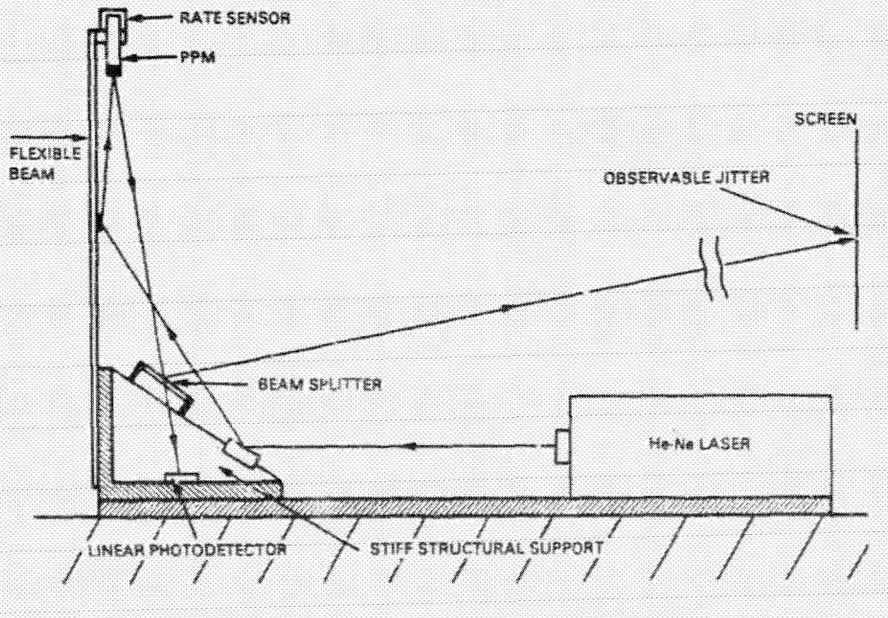

FIG. 2 BEAM CONTROL DIAGRAM

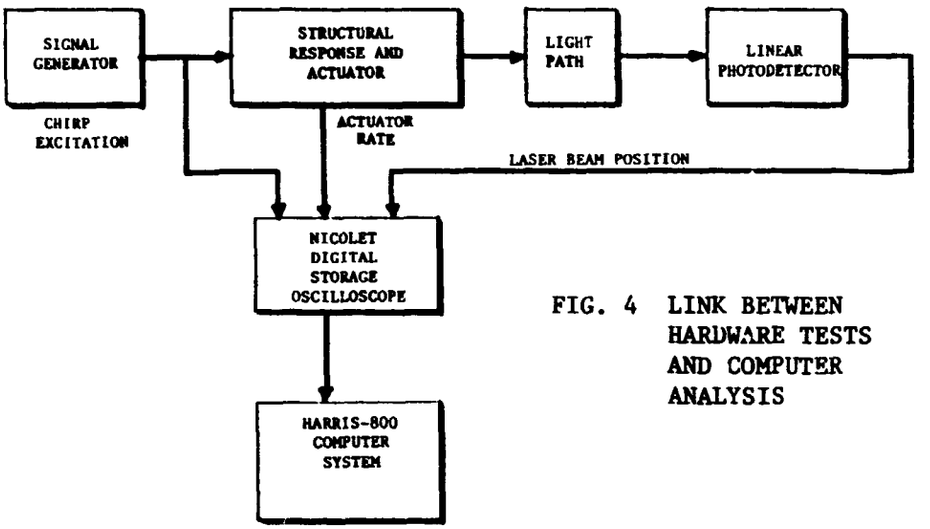

FIG. 4 LINK BETWEEN HARDWARE TESTS AND COMPUTER ANALYSIS

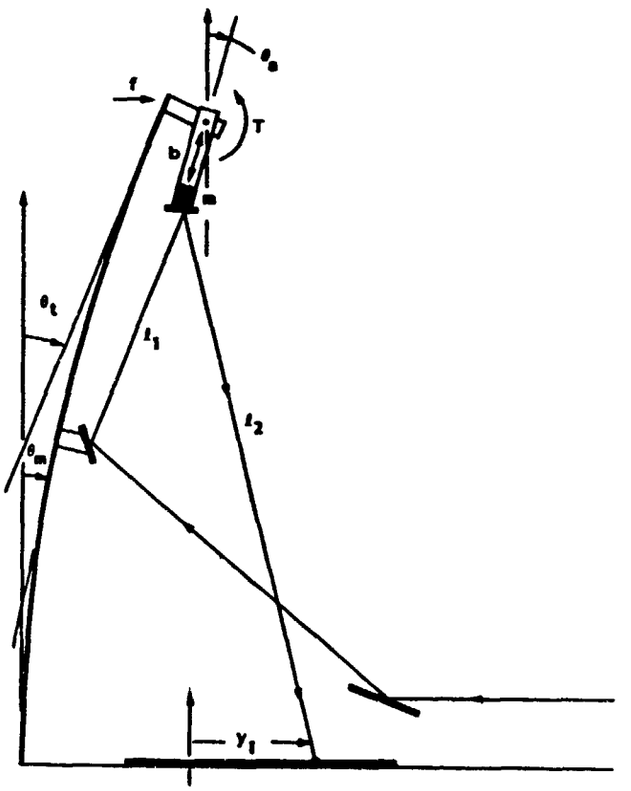

FIG. 5 BEAM EXPERIMENT GEOMETRY

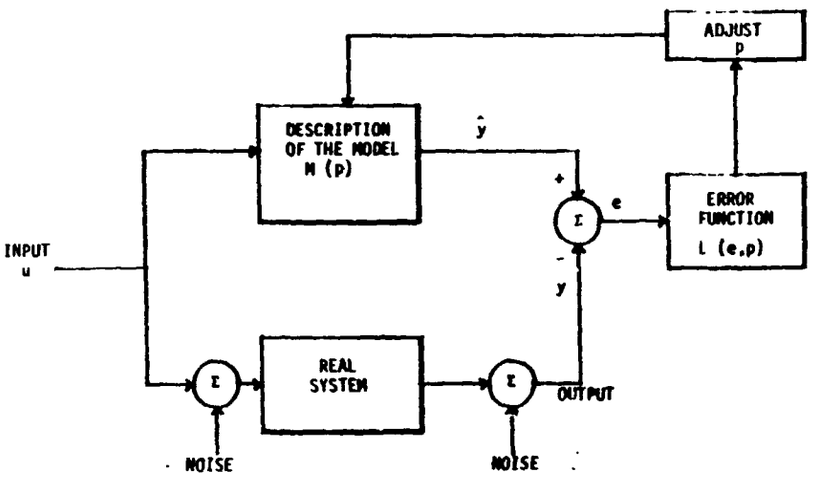

FIG. 6 COMPONENTS OF AN IDENTIFICATION SCHEME

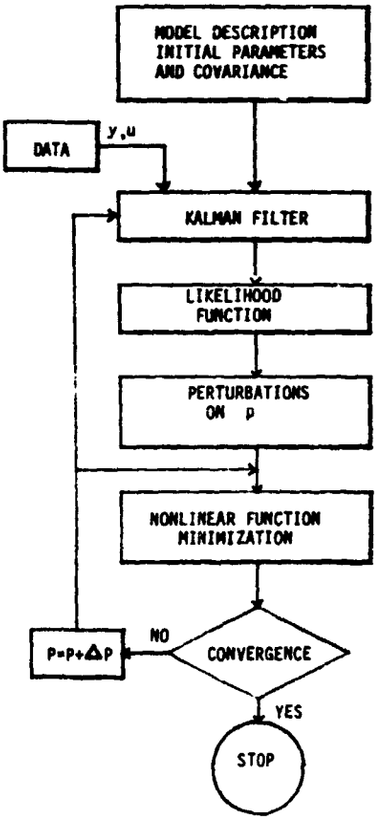

FIG. 7 COMPUTATIONS IN THE MLE

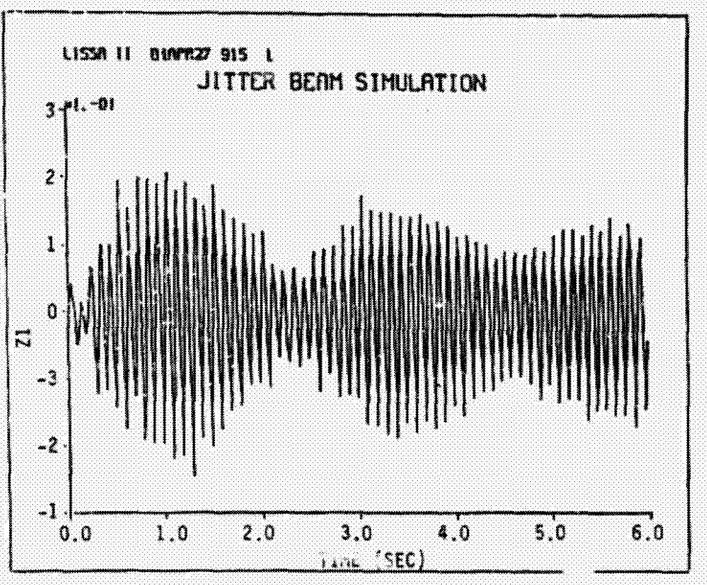

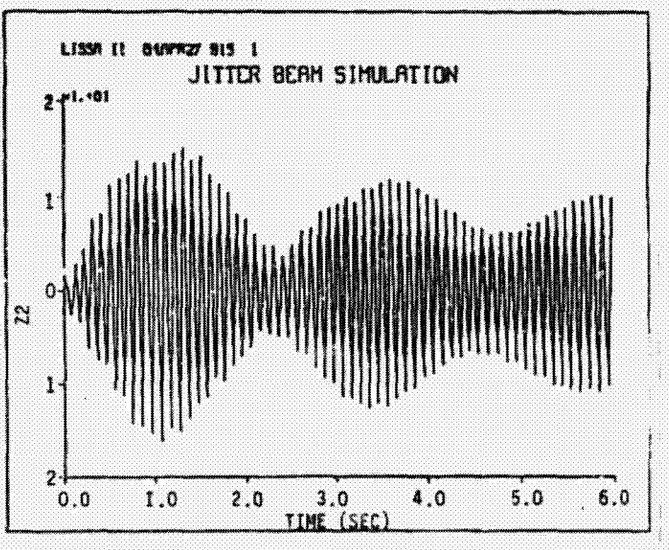

FIG. 8 BEAM POSITION AND RELATIVE ANGULAR RATE

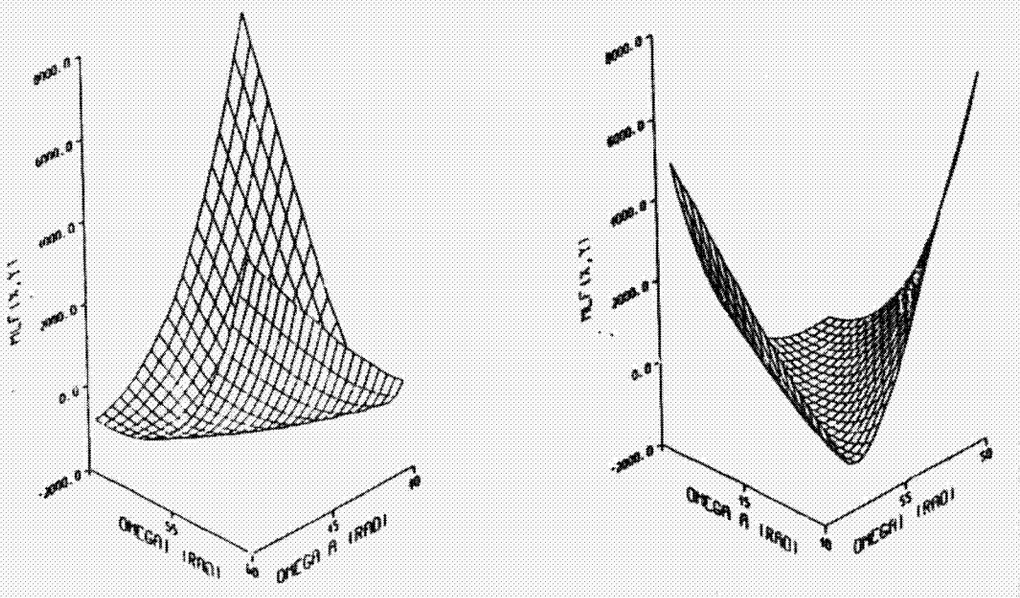

FIG. 9 MAXIMUM LIKELIHOOD SURFACE

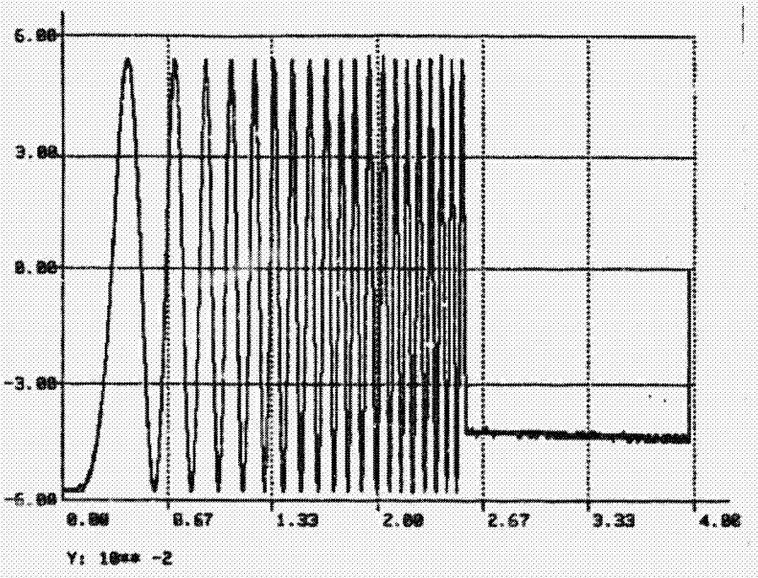

FIG. 10 BEAM EXCITATION INPUT

FIG. 11 COMPARISON BETWEEN ESTIMATED AND MEASURED OUTPUTS